Selective Raman Scattering from the Core Chlorophylls in Photosystem I via Preresonant Near-Infrared Excitation

David H. Stewart,[†,§] Agnes Cua,[‡] David F. Bocian,[*,‡] and Gary W. Brudvig[*,†]

Department of Chemistry, Sterling Chemistry Laboratory, Yale University, P.O. Box 208107, New Haven, Connecticut 06520-8107, and Department of Chemistry, University of California, Riverside, California 92521-0403

Received: November 11, 1998; In Final Form: February 16, 1999

The Raman scattering characteristics of photosystem I (PSI) over the 200−1700-cm^{-1} frequency range have been examined using near-infrared (NIR) excitation (λ_{ex} = 800 nm). The salient features observed in the spectra are as follows: (1) The Raman spectra are characteristic of neutral, pentacoordinate chlorophyll *a* (Chl *a*) molecules regardless of the oxidation state of the primary electron donor, P700. No Raman bands are observed for the oxidized primary donor, P700^{+}, despite the fact that the 800-nm excitation wavelength is coincident with a NIR absorption feature of the π-cation radical species. (2) The redox state of P700 has a strong influence on the temperature dependence of the preresonance Raman (PRR) scattering intensities of the neutral Chls in PSI (Q_y absorption maxima 660−720 nm). When P700 is neutral, the PRR intensities of the neutral Chls decrease approximately 4-fold on going from 77 to 200 K. When P700 is chemically or photochemically oxidized, the PRR scattering intensities of the neutral Chls are essentially temperature independent. The PRR intensities of the chemically oxidized sample at 77 K are approximately 50% larger than those of the neutral sample, whereas those at 200 K are about 4-fold larger and are comparable to those observed at 77 K. The observation that the redox state of P700 dramatically alters the PRR scattering intensities of the neutral Chls suggests that the dominant contribution to the PRR spectrum obtained with 800 nm excitation is from either neutral Chls that are electronically coupled to P700 or these molecules plus the neutral pair of Chls in P700. The structure of PSI indicates that the P700 dimer is in close proximity to only a handful of core monomeric Chls. Thus, these findings suggest that NIR-excitation PRR spectroscopy provides a selective probe of the core Chls in PSI and may aid in the characterization of the electronic coupling among these Chls.

Introduction

As more is revealed about the molecular structures of photosystem I (PSI) and photosystem II (PSII), the number of similarities between the two reactions centers becomes increasingly apparent.[1,2] Consequently, studies of either of the photosystems can impact interpretations of the other. Likewise, spectroscopic and structural information about PSI and PSII is commonly compared to their evolutionary predecessor, the structurally well-defined bacterial photosynthetic reaction center (BRC).[3] The reaction center cores of the BRC, PSI, and PSII are thought to be similar in that they contain a dimer of bacteriochlorophylls (BChls) or chlorophylls (Chls)—known as P870, P700, and P680, respectively—which serves as the primary electron donor in the photochemical charge separation. In addition to the primary donors, each of the photosynthetic complexes contains a group of four core monomeric chlorins (Chls, BChls, pheophytins (Pheos), or bacteriopheophytins (BPheos)), which participate in and facilitate the photochemical electron-transfer reactions. In recent years, significant effort has been exerted to define both the electronic structure and the excitation dynamics of the core BChls/Chls that participate in the primary photochemistry in the BRC, PSI, and PSII.[4]

There are also a large number of peripheral Chls/BChls associated with the BRC, PSI, and PSII that function to absorb light and transfer the excitation energy into the reaction center. In the case of the BRC and PSII, it is possible to separate the reaction center from the antenna proteins, and this has facilitated the application of optical spectroscopic methods to study the primary photochemical processes. In contrast, in PSI the core and peripheral antenna Chls are all bound to the psaA/psaB heterodimer and cannot be physically separated. Consequently, it is much more difficult to study the primary photochemistry of PSI by optical spectroscopy owing to the large background absorption from the peripheral antenna Chls.

One approach to obtaining information about the core BChls and Chls in the BRC, PSI, and PSII has been to use resonance Raman (RR) spectroscopy to identify molecular vibrations that reflect the structure and dynamics of these chromophores.[5] RR has been extensively applied to the BRC because it is the simplest of the three systems, containing a total of only six bacteriochlorins. Near-infrared (NIR) excitation RR studies of the BRC have been particularly fruitful because the different cofactors can be selectively interrogated due to the energetic separation of the absorption bands of the lowest-lying singlet excited states.[5c] RR studies involving NIR (and higher-energy) excitation have been used to assign the high-frequency (1400−

[†] Yale University.
[‡] University of California, Riverside.
[§] Current address: Xanthon, Inc., 104 Alexander Dr., Research Triangle Park, NC 27709.
* Corresponding authors. D.F.B.: phone, (909) 787-3660; Fax, (909) 787-4713; e-mail, dbocian@ucrac1.ucr.edu. G.W.B.: phone, (203) 432-5202; Fax, (203) 432-6144; e-mail, gary.brudvig@yale.edu.

10.1021/jp984409a CCC: $18.00
Published on Web 04/21/1999

1750 cm^{-1}) vibrational modes of P870, the two BPheos, and the two monomeric BChls in the BRC.[6] More recently, NIR-excitation RR studies in conjunction with ^{15}N and ^{26}Mg isotopic labeling have been used to make detailed assignments for the low-frequency (50−500 cm^{-1}) vibrations of these cofactors.[7] The characteristics of the lowest-lying singlet excited states of P870, the BChls, and the BPheos have been examined through studies of the temperature dependence of the RR intensities of each of these species[8,9] as well as through characterization of BRC mutants in which the coordination environment of P870 is altered to create a BChl−BPheo heterodimer in place of the BChl homodimer.[10,11] In the case of PSII, NIR-excitation RR spectroscopy has recently been utilized to identify the vibrational modes of a redox-active monomeric Chl cation, Chl_Z^+,[12] and to assign the axial ligand of this Chl.[13] Less work has been done toward RR characterization of PSI, although one report describes the influence of the oxidation state of P700 on the high-frequency Soret-excitation RR spectra of the PSI Chls at 15 K.[14]

In large part, RR studies of intact PSI and PSII complexes have been limited because of the significant spectral overlap among the many Chls (>35) bound to these proteins as well as the background interference from fluorescence that is emitted by these Chls. The latter difficulty can be mitigated using the technique shifted-excitation Raman difference spectroscopy (SERDS).[15,16] Thus far, SERDS has been used primarily to obtain structural, vibrational, and electronic information on the BChls and BPheos in the BRC,[7−11] although the method has recently been extended to the Chls in PSII.[12,13] The use of SERDS to study PSI and PSII is still limited, however, because it does not address the problem of spectral overlap. In the case of Chls that undergo oxidation, the NIR absorption bands associated with Chl π-cation radicals (∼800−850 nm) provide a way to circumvent this limitation. Excitation into these NIR absorption bands (which are at much longer wavelength than the Q_y absorption bands of the neutral Chls (660−720 nm)) permitted us to obtain RR spectra of the monomeric cation Chl_Z^+ with minimal interference from the large background of neutral Chls.[12,13]

The initial goal of the studies reported herein was to extend our NIR-excitation RR studies of Chl cations to $P700^+$ in PSI. As is the case for monomeric Chl cations, $P700^+$ exhibits a NIR absorption feature that is energetically well separated from the Q_y absorption bands of the neutral Chls (vide infra). Although our initial objective of directly probing $P700^+$ was not achieved, certain unexpected properties of PSI emerged during the course of collecting NIR-excitation Raman spectra. In particular, we observed a dramatic effect of the redox state of P700 on the preresonance Raman (PRR) scattering characteristics of the neutral Chls. This observation has important implications for the identity of the chromophores contributing to the PRR spectrum as well as the electronic coupling among these Chls. In this paper, we report on the unusual PRR scattering characteristics of the neutral Chls in PSI.

Experimental Section

Preparation of Photosystem I Core Complexes. Cells of *Synechocystis* were grown photoheterotrophically at 30 °C in 18-L carboys containing BG-11 medium[17] supplemented with 5 mM glucose and bubbled with 5% CO_2 in air. Aggregated PSI complexes were isolated from these cells using the procedure of Tang and Diner[18] and were stored in 50 mM MES, pH 6.0, 20 mM $CaCl_2$, 10 mM NaCl, 20% (v/v) glycerol, and 0.03% *n*-dodecyl β-D-maltoside at 77 K in the dark until further use. Determinations of the Chl concentration were made by extraction into methanol and using ϵ_{665} = 79.24 mL/(mg of Chl cm) for Chl *a* in methanol.[19]

Optical and EPR Spectroscopy. Optical spectra of the NIR absorption band of $P700^+$ were collected using a Perkin-Elmer Lambda 6 UV/vis spectrophotometer. The measurements were made at 77 K by using a home-built Plexiglas flat cell (path length ∼1/32 in.) as described previously.[13] The samples were frozen as uncracked glasses, and condensation buildup on the quartz surface was prevented by a flow of dry N_2 gas. Both nonilluminated and 77 K-illuminated spectra were collected for untreated PSI and for 5 mM potassium ferricyanide-treated PSI; illumination consisted of 15−18 min of continuous white light from a 100 W quartz/halogen lamp at 77 K. The PSI samples were at a concentration of 5.8 mg of Chl/mL in 50 mM MES, pH 6.0, 20 mM $CaCl_2$, 10 mM NaCl, 40% (v/v) glycerol. Cryogenic EPR spectra were collected on a Varian E-line EPR spectrometer equipped with an Oxford Instruments ESR 900 liquid helium cryostat. The spectrometer conditions were as follows: microwave frequency, 9.28 GHz; microwave power, 0.03 mW; magnetic field modulation amplitude, 2 G; temperature, 30 K. These conditions are nonsaturating for the $P700^+$ EPR signal. The maximum yield of photooxidized $P700^+$ was obtained by freezing an untreated PSI (∼0.5 mg of Chl/mL) sample to 200 K in a dry ice/acetone bath over ∼3 min while continuously illuminating the sample with a 100-W quartz/halogen lamp. The stability of $P700^+$ at 200 K was determined by measuring the integrated area of the narrow radical EPR signal periodically during a timed incubation at 200 K.

Raman Spectroscopy. The Raman measurements were made at 200 and 77 K on highly concentrated, glassy samples contained in 1-mm i.d. capillary tubes. The PSI samples were at a concentration of about 20 mg of Chl/mL in 50 mM MES, pH 6.0, 20 mM $CaCl_2$, 10 mM NaCl, 20% (v/v) glycerol. The sampling accessories, spectrometer, and laser systems have been previously described.[6,20] Each Raman data set was obtained with 2 h of signal averaging. Cosmic spikes in the individual scans were removed prior to coaddition of the scans. The spectral resolution was ∼2 cm^{-1}. The laser power was ∼5 mW. All spectra are unpolarized. The spectral data were calibrated using the known frequencies of fenchone. Both nonilluminated and illuminated spectra were collected for untreated PSI; only nonilluminated spectra were collected for 4 mM potassium ferricyanide-treated PSI. Illumination consisted of exposure to continuous white light from a focused 200-W quartz/halogen lamp while freezing to the desired data collection temperature (either 200 or 77 K). For all three sample types (nonilluminated untreated, ferricyanide treated, illuminated untreated), the Raman data were acquired under identical conditions (sample concentration, laser power, data acquisition time, and spectral slit width (see above for values)).

All of the Raman spectra were acquired using the SERDS technique in order to reduce the level of interference from fluorescence.[15,16] The application of the SERDS method to photosynthetic proteins has been previously described in detail.[7,8,10,15,16,21] Briefly, each data set is acquired at two excitation wavelengths that differ by a small wavenumber increment (typically 10 cm^{-1}). [The 2-h data acquisition time indicated above is for each of the two data sets required to construct a SERDS trace.] These data sets are subtracted to yield a background-free difference (SERDS) spectrum. The Raman data presented herein were obtained by subtracting the initial spectrum from the shifted spectrum. The spectral window is defined by the initial spectrum and corresponds to the wave-

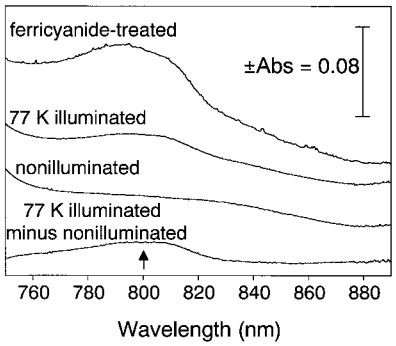

Figure 1. Absorption spectra of ferricyanide-treated (top trace) and untreated PSI in the NIR. The second, third, and bottom traces are 77 K-illuminated, nonilluminated, and 77 K-illuminated-minus-nonilluminated spectra of untreated PSI, respectively. The broad cation absorption band of $P700^+$ is visible at ~800 nm in the top, second, and bottom traces. The spectra are vertically shifted for clarity. The arrow indicates the excitation wavelength used to obtain the PRR data.

number axis in the figures. The normal Raman spectrum is then reconstructed from the SERDS data by fitting the latter to a series of derivative-shaped functions (in this case, difference bands generated from Gaussian functions) of arbitrary frequency, amplitude, and width. The frequencies marked in the figures correspond to the positions of the bands used in the fits and, thus, do not necessarily correspond to the peak maxima for overlapping bands. In addition, certain bands are marked that are not clearly resolved in the spectra. These bands are indicated because their inclusion noticeably improved the quality of the fits to the SERDS data based on the residuals (observed spectra minus fits).

Results

Optical and EPR Characterization of $P700^+$. As noted above, our initial goal was to obtain RR spectra of $P700^+$ using selective excitation into the NIR absorption band of the cation. $P700^+$ is stably trapped in PSI by either photochemical (low-temperature illumination) or chemical (ferricyanide treatment) oxidation. The NIR absorption feature characteristic of this cation is shown in Figure 1. This absorption band represents a weak electronic transition and requires a high sample concentration to be observed. In addition, the absorption band is very broad, making it difficult to determine λ_{max} exactly. The $P700^+$ NIR absorption band appears to maximize around 800 nm; therefore, 800 nm (indicated with an arrow in the figure) was selected as the primary excitation wavelength for the Raman measurements. The yield of $P700^+$ obtained by illumination at 77 K (bottom trace) is about 35% of that attained by chemical oxidation (top trace) or by freezing under illumination to $\leq$200 K. As a result, the two latter methods were used to generate $P700^+$ for the Raman experiments. One concern was the stability of photooxidized P700 at 200 K over the course of the RR experiment (4 h). Any significant changes in the redox state of P700 were ruled out by monitoring the decay of the $P700^+$ EPR signal generated by freezing PSI to 200 K under continuous illumination. The $P700^+$ EPR signal was completely unaffected by a 40-min incubation at 200 K.

Raman Characterization of Photosystem I. NIR-excitation Raman spectra of PSI obtained at two temperatures, 200 and 77 K, are shown in Figures 2−4. The three panels of each figure include spectra of three sample types: two spectra of PSI in which P700 is oxidized (ferricyanide-treated PSI and illuminated-untreated PSI) and one spectrum in which P700 is neutral (nonilluminated-untreated PSI). The data shown were

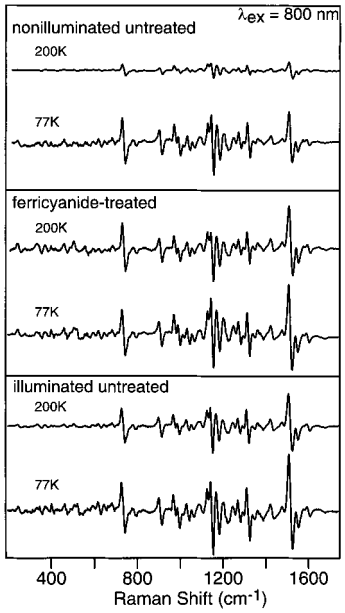

Figure 2. NIR-excitation (λ_{ex} = 800 nm) SERDS data obtained for nonilluminated-untreated (top panel), ferricyanide-treated (middle panel), and illuminated-untreated (bottom panel) PSI at 200 and 77 K. P700 is neutral in the spectra shown in the top panel and oxidized in the spectra shown in the middle and bottom panels.

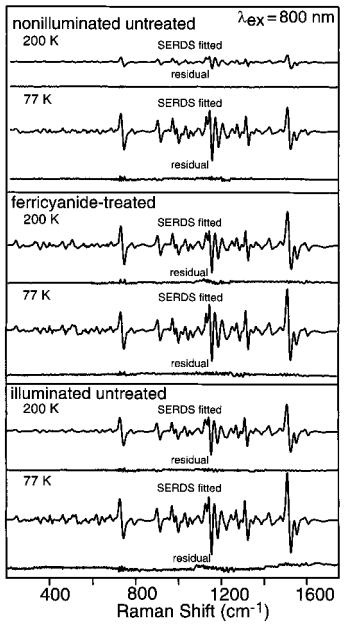

Figure 3. Fits of the NIR-excitation (λ_{ex} = 800 nm) SERDS data for nonilluminated-untreated (top panel), ferricyanide-treated (middle panel), and illuminated-untreated (bottom panel) PSI at 200 and 77 K. The residuals obtained by subtracting the fits from the raw SERDS data shown in Figure 2 are also shown beneath each fitted SERDS trace.

obtained in four ~450-cm^{-1} wide overlapping spectral windows. Figure 2 compares the raw (unsmoothed) SERDS traces obtained with λ_{ex} = 800 nm for the three sample types at 200 and 77 K. Figure 3 shows the fits of the raw SERDS data sets shown in Figure 2 along with the residuals for the fits (observed minus fitted data). The relatively small residuals compared with the SERDS intensities in Figure 3 are indicative of the excellent fidelity of the fits for all three PSI sample types at both 200 and 77 K. Figure 4 shows the Raman spectra reconstructed from the SERDS fits for ferricyanide-treated and illuminated- and

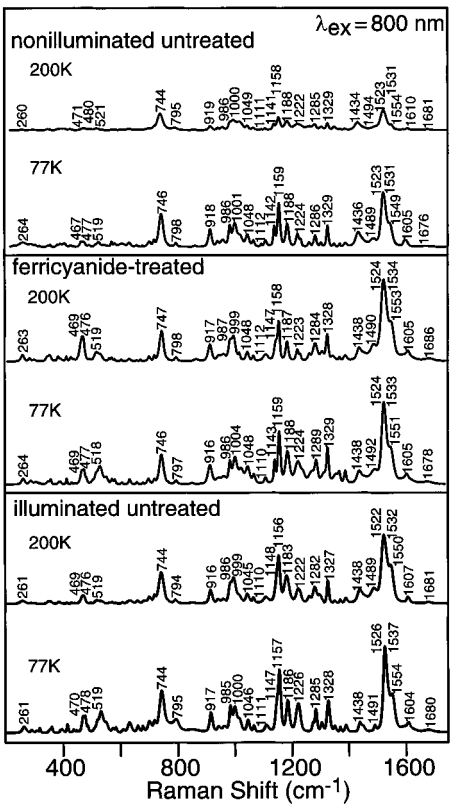

Figure 4. Comparison of the NIR-excitation (λ_{ex} = 800 nm) Raman spectra of PSI reconstructed from the fits to the SERDS data (Figure 3) for the nonilluminated-untreated (top panel), ferricyanide-treated (middle panel), and illuminated-untreated (bottom panel) samples at 200 and 77 K. P700 is neutral in the spectra shown in the top panel and oxidized the spectra shown in the middle and bottom panels.

nonilluminated-untreated PSI at 200 and 77 K. Certain weaker Raman bands are not marked in Figure 4 for pictorial clarity.

The Raman spectra for the different PSI samples shown in Figures 2−4 were obtained without an internal intensity standard; thus, the absolute Raman cross sections cannot be determined. However, all sampling and data acquisition conditions were identical for the three types of samples (vide supra). Thus, the relative Raman intensities for the different samples shown in a given figure are reasonably faithful representations of the actual relative intensities (within ∼10%, based on comparison of multiple data sets for each type of sample). The Raman intensities for the spectra shown in different figures cannot be compared with one another because they are plotted on different scales to facilitate presentation.

The salient features of the Raman spectra shown in Figures 2−4 can be summarized as follows:

(1) No new Raman bands are observed upon formation of $P700^+$. For all three samples at both temperatures, the Raman spectra are exclusively characteristic of neutral Chl *a*, despite the fact that the 800 nm excitation wavelength is coincident with the NIR absorption feature of $P700^+$. This assignment is indicated by a comparison of the reconstructed spectra shown in Figure 4 with the Q_y-excitation RR spectra collected from film aggregates of Chl *a* at 15 K.[22] In particular, isolated Chl *a* exhibits RR bands at 261, 469, 518, 746, 800, 914, 986, 1046, 1114, 1146, 1188, 1222, 1286, 1328, 1524, and 1553 cm^{-1} that agree quite closely with the PSI bands at 261−264, 469−471, 518−521, 744−747, 794−798, 916−919, 985−987, 1045−1049, 1110−1112, 1141−1148, 1183−1188, 1222−1226, 1282−1289, 1327−1329, 1522−1526, and 1549−1554 cm^{-1}. We also note that our previous NIR-excitation RR studies of Chl_Z^+ have shown that Chl cations exhibit a strong band near 1501 cm^{-1}.[12,13] No hint of such a feature is observed in the Raman spectra of oxidized PSI. Finally, we note that the frequencies of the ring-skeletal modes of the neutral Chls in PSI (in particular those at ∼1552 and ∼1533 cm^{-1}) are characteristics of pentacoordinate species (single axial ligand to the Mg(II) ion).[23]

TABLE 1: Relative PRR Intensities for the PSI Samples[a]

	nonilluminated untreated	ferricyanide treated	illuminated untreated
77 K	1.0	1.5	1.5
200 K	0.3	1.5	1.3

[a] The intensities are based on the peak height of the Raman feature observed in the 1527−1532-cm^{-1} region. The intensity of this feature in the spectrum of the nonilluminated-untreated sample at 77 K is arbitrarily taken as unity.

(2) The redox state of P700 has a strong influence on the temperature dependence of the PRR scattering intensities of the neutral Chls in PSI. [The Raman spectra acquired with λ_{ex} = 800 nm are most appropriately designated PRR spectra because the Q_y absorption maxima of the neutral chromophores fall at significantly shorter wavelengths (660−720 nm).] In particular, when P700 is neutral (nonilluminated-untreated PSI), the PRR intensities decrease approximately 4-fold on going from 77 to 200 K. The magnitude of the decrease in PRR intensity is generally similar (but not identical) for the different Raman bands. When P700 is chemically or photochemically oxidized, the PRR scattering intensities of the neutral Chls are essentially temperature independent. The PRR intensities of the chemically oxidized sample at 77 K are approximately 50% larger than those of the neutral sample, whereas those at 200 K are about 4-fold larger and are comparable to those observed at 77 K. The PRR intensities in the photochemically oxidized sample appear to be somewhat more sensitive to temperature than those of the chemically oxidized sample. However, this observation is attributed to the presence of residual neutral P700 in the former sample rather than a difference in behavior for the samples generated by the two types of oxidation. The PRR intensities observed for the three sample types at the two temperatures are summarized in Table 1. The values shown in the table are based on the behavior of the most intense PRR feature whose centroid is observed in the 1527−1532-cm^{-1} range. The intensity of this feature for the nonilluminated-untreated sample at 77 K is arbitrarily taken as unity.

The Raman scattering characteristics exhibited by PSI prompted us to undertake a series of additional experiments. (1) The excitation wavelength was tuned in ∼10-nm intervals through the 790−830-nm region. At all excitation wavelengths, the same spectral features are observed. However, the total Raman intensity falls off slowly as the exciting line is shifted to longer wavelength and increases slowly as the exciting line is shifted to shorter wavelength. These observations are further consistent with the scattering arising from the PRR intensity from the neutral Chls. (2) The temperature was cycled between 77 and 200 K for the different samples. For the nonilluminated sample containing neutral P700, the PRR intensities cycled up and down, reproducing the results shown in the figures for the two temperatures. For the chemically oxidized samples containing $P700^+$, little or no changes in PRR intensities were observed upon temperature cycling, again consistent with the data shown in the figures.

Discussion

The NIR-excitation Raman scattering characteristics of PSI provide insights into the structural and electronic properties of

the Chl *a* chromophores as well as the nature of interchromophore interactions. The vibrational frequencies of the Chls reflect the structural properties of the molecules in the ground electronic state, whereas the Raman intensities contain information concerning the dynamics in the excited electronic states.[24] For PSI, the vibrational frequencies observed for the neutral Chls are in all respects typical of those of isolated Chl *a*.[22] The frequencies give no indication of any unusual structural characteristics that might be associated with the chromophores in the protein. On the other hand, the Raman intensities exhibit certain unusual features, namely the absence of observable RR scattering from $P700^+$ and the temperature dependence of the PRR scattering from the neutral Chls. In the sections below, we address each of these issues in turn and discuss their implications for the identity of the chromophores contributing to the Raman spectrum and electronic properties of these chromophores.

The absence of any observable NIR-excitation RR scattering from $P700^+$ could potentially be due to the fact that the 800-nm absorption feature of this cation is relatively weak and broad, resulting in a low RR cross section. However, our recent RR studies of Chl_Z^+ in PSII argue against this interpretation. In particular, Chl_Z^+ exhibits a NIR absorption band that is comparable in intensity and breadth to that of $P700^+$.[12,13] Yet Chl_Z^+ exhibits RR scattering that is readily observable above the background PRR scattering from the neutral Chls. At this time, the assignments of the NIR absorption bands are not certain for either Chl_Z^+ or $P700^+$, and it is possible that the nature of the electronic transition is different for the two types of cations. If so, both the Franck−Condon overlaps and/or the excited-state dynamics and, hence, the RR cross sections could also be appreciably different. The highly damped RR cross section for $P700^+$ would imply either very small Franck−Condon overlaps and/or the existence of an ultrafast (fs) excited-state dephasing channel. Given that the NIR absorption bands of $P700^+$ and Chl_Z^+ are qualitatively similar in breadth, it seems unlikely that a difference in Franck−Condon factors alone could account for the very large difference in RR cross section for the two types of cation. Consequently, we favor an interpretation wherein the RR cross section of $P700^+$ is damped by an ultrafast dephasing process that is unique to the dimeric architecture of the primary electron donor.

The damping of the RR cross section of $P700^+$ via ultrafast dephasing has precedence in two previous observations. (1) The absolute RR cross section for the lowest-energy transition of the neutral P870 dimer in the BRC has been shown to be substantially smaller than that of the Q_y transitions of the neutral monomeric BChls.[9] The highly damped RR cross section for P870 has been attributed to ultrafast dephasing (<50 fs) that is unique to the dimer. (2) Previous RR studies of oxidized lanthanide sandwich porphyrin dimers have shown that excitation of the NIR absorption bands of these complexes produces minimal RR scattering, despite the fact that the NIR absorption features have substantial oscillator strength.[25,26] The lanthanide sandwich porphyrin dimers are very strongly electronically coupled due to complete face-to-face overlap and close interring separation. It has been proposed that the poor RR scattering characteristics of the NIR electronic transitions of the sandwich porphyrin dimers arise because the strong $\pi\pi$ interactions lead to rapid dephasing, which in turn damps the RR cross section.[26] In the case of $P700^+$, a similar ultrafast dephasing mechanism together with the low oscillator strength of the NIR electronic transition could render any RR scattering too weak to be observed.

The strong temperature dependence of the PRR scattering intensities of the neutral Chls in PSI can also be explained in terms of an ultrafast (femtosecond) dephasing process. This dephasing process effectively competes with the scattering process at 200 K, but not at cyrogenic temperatures. The fact that formation of $P700^+$ increases the PRR scattering intensities of the neutral Chls and effectively eliminates the strong temperature dependence of these intensities clearly signals the involvement of the dimer in the dephasing process. The nature of this involvement will be discussed further below. The observation that the oxidation state of P700 influences the Raman scattering characteristics of the neutral Chls has precedence in previous studies of the BRC. In particular, RR studies of *Rhodobacter capsulatus* reaction centers at 200 K have shown that the RR cross section of the carotenoid (Car), sphaeroidenone, is strongly influenced by the oxidation state of P870.[27] Upon formation of $P870^+$, the RR cross section of the Car increases by a factor of 2 or more. This effect was explained in terms of coupling of the S_2 excited state of the Car with the Q_x excited state(s) of P870. When P870 is neutral, Car (S_2) and P870 (Q_x) are nearly isoenergetic. This property facilitates electronic coupling between the Car and P870, which opens an ultrafast dephasing channel that damps the RR cross section of the Car. Formation of $P870^+$ shifts the energy of the Q_x excited state(s) of the primary donor, thereby reducing the electronic coupling and closing the dephasing channel, which in turn increases the RR cross section of the Car. The similar effects of primary donor oxidation state on the Raman scattering characteristics of the neutral Chls in PSI and the Car in the BRC suggest that electronic coupling pathways among the Chls in PSI open new ultrafast dephasing channels.

One key question that remains is the identity of the neutral Chls that contribute to the PRR spectrum of PSI. The fact that oxidation of P700 alters the PRR scattering suggests that the neutral dimer may contribute to the spectrum. However, P700 cannot be the sole contributor to the PRR spectrum because PRR scattering is observed from neutral Chls after formation of $P700^+$. The fact that the Raman cross section of the neutral Chls *increases* upon formation of $P700^+$ precludes the determination of whether P700 contributes to the PRR spectrum at all or whether the scattering arises exclusively from the other neutral Chls in PSI. It is also possible that both P700 and the other neutral Chls contribute to the PRR spectrum when the primary donor is neutral and that only the latter neutral Chls contribute when P700 is oxidized.

The fact that oxidation of P700 significantly alters the PRR scattering intensity measured at 200 K strongly suggests that neutral Chls that are electronically coupled to P700 are key contributors to the spectra. The substantially larger PRR intensity observed for the samples containing $P700^+$ versus P700 further suggests that this group of neutral Chls completely dominates the scattering (at both 200 and 77 K) for samples containing $P700^+$. These same neutral Chls that are electronically coupled to the primary donor also dominate the 77 K PRR spectrum of the sample containing P700 (although P700 may also contribute, vide supra). The relatively weak PRR scattering observed for this sample at 200 K could also be entirely due to this group of neutral Chls. However, we cannot rule out the possibility that some portion of this residual scattering originates from neutral Chls different from those that contribute to the PRR spectrum under the other conditions (cryogenic temperatures or formation of $P700^+$).

The logical candidates for the group of neutral Chls that are electronically coupled to P700 are the cofactors that are in

closest proximity to this center. Inspection of the X-ray crystallographic structure of PSI from the cyanobacterium, *Synechococcus elongatus*,[1] indicates that there is a core of six Chls (including P700) in which none of the Chls is farther than 6 Å (edge-to-edge) from at least one other Chl. There are also two "connecting" Chls that are within ~9 Å (edge-to-edge) of Chls at the edge of the core. The remaining Chls are substantially further away and are much less likely to be electronically coupled to P700 or the core Chls. The likelihood that only a small number of neutral Chls dominate the NIR-excitation PRR spectrum of PSI is further supported by the observation that the Raman bands are relatively narrow and similar to those observed for isolated Chl *a*.[22] If a large number of neutral Chls were contributing to the PRR spectrum, it might be expected that the Raman bands would be broader owing to some degree of heterogeneity in the local environment around the different pigments.

Based on the significant effect of the oxidation state of P700 on the PRR spectrum of the neutral Chls in PSI and the likelihood that P700 is electronically coupled to only a few additional Chls, it appears that the NIR-excitation PRR spectrum of PSI is highly selective for the core Chls in the protein. There are a number of possible explanations for this finding. One possibility is that the 800 nm excitation wavelength favors the more red absorbing Chls in PSI and that the core Chls make up a significant proportion of these lower-energy Chls. However, there must be some spectral overlap between the red-absorbing core Chls and other red-absorbing Chls in PSI. Interestingly, the nature of red-absorbing Chls in PSI is currently a topic of debate with regard to both the structure and location of these species as well as their role in energy transfer.[28,29] Thus, NIR-excitation PRR studies may provide new insight toward elucidating the function of the red-absorbing Chls in PSI. Another explanation for the selectivity of NIR excitation PRR spectroscopy for the core Chls is that the Raman scattering cross section of this group of Chls might be inherently larger than that of the other Chls in PSI. An enhanced Raman scattering cross section might result if the core Chls behave as a supermolecular aggregate. In this regard, Parkash et al. have recently reported unusual scattering characteristics from electronically coupled Chl aggregates.[30] In PSI, such an array of electronically coupled core Chls would logically include P700. Thus, oxidation of P700 would be expected to influence the excited-state dephasing processes, which under certain conditions compete effectively with Raman scattering. A change in the redox state of the primary donor in PSI would result in an energy mismatch between the excited-state(s) of this chromophore and those of the other core neutral Chls, thereby altering the excited-state surface of the coupled system. The group of core neutral Chls that remains upon formation of $P700^+$ must, however, constitute an electronically coupled subsystem that also has an enhanced Raman scattering cross section (as is evidenced by the fact that these neutral Chls appear to dominate the PRR spectrum when P700 is oxidized and electronically decoupled from the subgroup of core Chls). The implication of all of the above-noted observations is that there are multiple electronic coupling pathways among the core Chls in PSI and that these couplings are modulated by the oxidation state of the primary electron donor.

Conclusions

In this study, we have used NIR-excitation Raman spectroscopy to probe the neutral Chls in PSI. The extension of NIR Raman techniques to PSI is important because it provides structural and electronic information about Chls that have been previously less well characterized owing to severe spectral overlap and large fluorescence backgrounds. Two key findings of this study are that $P700^+$ exhibits very poor NIR-excitation RR scattering characteristics and that the PRR spectrum of PSI appears to be dominated by only a small group of core Chls that may include the primary electron donor. Together, these observations suggest the presence of electronic coupling pathways among the core Chls that should be amenable to direct examination via ultrafast coherent spectroscopic methods. Finally, the observation that the NIR-excitation PRR spectrum of PSI is dominated by the core Chls affords a clear means of examining the structural and electronic properties of the key cofactors that are involved in the primary electron-transfer process. Future NIR-excitation PRR studies of PSI will address this issue in more detail.

Acknowledgment. This work was supported by grants GM 39781 (D.F.B.) and GM 32715 (G.W.B.) from the National Institutes of Health, grant 96-35306-3398 (G.W.B.) from the National Research Initiative Competitive Grants Program/USDA, and by a National Institutes of Health predoctoral traineeship, GM 08283 (D.H.S.). We thank Prof. John Hartwig for the use of the Lambda 6 UV/vis spectrophotometer. We also appreciate helpful discussions with Profs. Warren Beck and Rienk van Grondelle.

References and Notes

(1) Schubert, W. D.; Klukas, O.; Krauss, N.; Saenger, W.; Fromme, P.; Witt, H. T. *J. Mol. Biol.* **1997**, *272*, 741.

(2) (a) Rhee, K.-H.; Morris, E. P.; Zheleva, D.; Hankamer, B.; Kühlbrandt, W.; Barber, J. *Nature (London)* **1997**, *389*, 522. (b) Rhee, K.-H.; Morris, E. P.; Barber, J.; Kühlbrandt, W. *Nature (London)* **1998**, *396*, 283.

(3) (a) Ermler, U.; Fritzsch, G.; Buchanan, S.; Michel, H. *Structure* **1994**, *2*, 925. (b) Deisenhofer, J.; Epp, O.; Sinning, I.; Michel, H. *J. Mol. Biol.* **1995**, *246*, 429. (c) Yeates, T. O.; Komiya, H.; Chirino, A.; Rees, D. C.; Allen, J. P.; Feher, G. *Proc. Natl. Acad. Sci. U.S.A.* **1988**, *85*, 7993. (d) El-Kabbani, O.; Chang, C.-H.; Tiede, D.; Norris, J.; Schiffer, M. *Biochemistry* **1991**, *30*, 5361.

(4) (a) *The Photosynthetic Reaction Center*; Deisenhofer, J., Norris, J. R., Eds.; Academic: San Diego, CA; 1993; Vol. II. (b) *Anoxygenic Photosynthetic Bacteria*; Blankenship, R. E., Madigan, M. T., Bauer, C. E., Eds.; Kluwer Academic Publishers: Dordrecht, The Netherlands, 1995; pp 503−708. (c) *The Reaction Center of Photosynthetic Bacteria*; Michel-Beyerle, M. E., Ed.; Springer: Berlin, Heidelberg, 1996. (d) van Grondelle, R.; Dekker, J. P.; Gillbro, T.; Sundstrum, V. *Biochim. Biophys. Acta* **1994**, *1187*, 1. (e) Greenfield, S. R.; Wasielewski, M. R. *Photosyn. Res.* **1996**, *48*, 83. (f) DiMago, L.; Chan, C.-K.; Jia, Y.; Lang, M.; Newman, R. R.; Mets, L.; Fleming, G. R.; Haselkorn, R. *Proc. Natl. Acad. Sci. U.S.A.* **1995**, *92*, 2725. (g) White, N. T. H.; Beddard, G. S.; Thorne, J. R. G.; Feehan, T. M.; Keyes, T. E.; Heathcote, P. *J. Phys. Chem.* **1996**, *100*, 12086. (h) Kumazaki, S.; Ikegami, I.; Yoshihara, K. *J. Phys. Chem. A* **1997**, *101*, 597.

(5) For reviews see: (a) Lutz, M.; Robert, B. In *Biological Applications of Raman Spectroscopy*; Spiro, T. G., Ed.; Wiley: New York, 1988; Vol. 3, pp 347−411. (b) Lutz, M.; Mäntele, W. In *Chlorophylls*; Scheer, H., Ed.; CRC Press: Boca Raton, FL, 1991; pp 855−902. (c) Lutz, M. *Biospectroscopy* **1995**, *1*, 313.

(6) Palaniappan, V.; Martin, P. C.; Chynwat, V.; Frank, H. A.; Bocian, D. F. *J. Am. Chem. Soc.* **1993**, *115*, 12035.

(7) (a) Czarnecki, K.; Diers, J. R.; Chynwat, V.; Erickson, J. P.; Frank, H. A.; Bocian, D. F. *J. Am. Chem. Soc.* **1997**, *119*, 415. (b) Czarnecki, K.; Chynwat, V.; Erickson, J. P.; Frank, H. A.; Bocian, D. F. *J. Am. Chem. Soc.* **1997**, *119*, 2594.

(8) Cherepy, N. J.; Shreve, A. P.; Moore, L. J.; Boxer, S. G.; Mathies, R. A. *J. Phys. Chem. B* **1997**, *101*, 3250.

(9) Cherepy, N. J.; Shreve, A. P.; Moore, L. J.; Boxer, S. G.; Mathies, R. A. *Biochemistry* **1997**, *36*, 8559.

(10) Palaniappan, V.; Schenck, C. C.; Bocian, D. F. *J. Phys. Chem.* **1995**, *99*, 17049.

(11) Laporte, L. L.; Palaniappan, v.; Davis, D. G.; Kirmaier, C.; Schenck, C. C.; Holten, D.; Bocian, D. F. *J. Phys. Chem.* **1996**, *100*, 17696.

(12) Cua, A.; Stewart, D. H.; Brudvig, G. W.; Bocian, D. F. *J. Am. Chem. Soc.* **1998**, *120*, 4532.

(13) Stewart, D. H.; Cua, A.; Chisholm, D. A.; Diner, B. A.; Bocian, D. F.; Brudvig, G. W. *Biochemistry* **1998**, *37*, 10040.
(14) Moënne-Loccoz, P.; Robert, B.; Ikegami, I.; Lutz, M. *Biochemistry* **1990**, *29*, 4740.
(15) Shreve, A. P.; Cherepy, N. J.; Franzen, S.; Boxer, S. G.; Mathies, R. A. *Proc. Natl. Acad. Sci. U.S.A.* **1991**, *88*, 11207.
(16) Shreve, A. P.; Cherepy, N. J.; Mathies, R. A. *Appl. Spectrosc.* **1992**, *46*, 707.
(17) Rippka, R.; Deruelles, J.; Waterbury, J. B.; Herdman, M.; Stanier, R. Y. *J. Gen. Microbiol.* **1979**, *111*, 1.
(18) Tang, X.-S.; Diner, B. A. *Biochemistry* **1994**, *33*, 4594.
(19) Lichtenthaler, H. K. *Methods Enzymol.* **1987**, *148*, 350.
(20) Palaniappan, V.; Aldema, M. A.; Frank, H. A.; Bocian, D. F. *Biochemistry* **1992**, *31*, 11050.
(21) Cherepy, N. J.; Shreve, A. P.; Moore, L. J.; Franzen, S.; Boxer, S. G.; Mathies, R. A. *J. Phys. Chem.* **1994**, *98*, 6023.
(22) Zhou, C.; Diers, J. R.; Bocian, D. F. *J. Phys. Chem. B* **1997**, *101*, 9635.
(23) Tasumi, M.; Fujuwara, M. *J. Phys. Chem.* **1986**, *90*, 250.
(24) Myers, A. B.; Mathies, R. A. In *Biological Applications of Raman Spectroscopy*; Spiro, T. G., Ed.; Wiley: New York, 1987; pp 1−58.
(25) Perng, J.-H.; Duchowski, J. K.; Bocian, D. F. *J. Phys. Chem.* **1991**, *95*, 1319.
(26) Martin, P. C.; Arnold, J.; Bocian, D. F. *J. Phys. Chem.* **1993**, *97*, 1332.
(27) Palaniappan, V.; Bocian, D. F. *Biochemistry* **1995**, *34*, 11106.
(28) Karapetyan, N. V.; Dorra, D.; Schweitzer, G.; Bezsmertnaya, I. N.; Holtzwarth, A. R. *Biochemistry* **1997**, *36*, 13830.
(29) Palsson, L. O.; Flemming, C.; Gobets, B.; van Grondelle, R.; Dekker, J. P.; Schlodder, E. *Biophys. J.* **1998**, *74*, 2611.
(30) Parkash, J.; Robblee, J. H.; Agnew, J.; Gibbs, E.; Collings, P.; Pasternack, R. F.; de Paula, J. C. *Biophys. J.* **1998**, *74*, 2089.